J. Fluid Mech. (1982), *vol.* 118, *pp.* 221–239
Printed in Great Britain

A theoretical and experimental study of the capsize of Salter's duck in extreme waves

By M. GREENHOW, T. VINJE,

Division of Marine Hydrodynamics, Norwegian Institute of Technology, Trondheim, Norway

P. BREVIG

Division of Ship and Ocean Laboratories, Norwegian Hydrodynamic Laboratories, Trondheim, Norway

AND J. TAYLOR

Wave Power Group, Department of Mechanical Engineering, University of Edinburgh, Scotland

(Received 22 October 1981)

This paper examines the problem of the survival of Salter's duck wave-energy device in extreme waves, both experimentally in a narrow tank at Edinburgh University and theoretically, using programs originally designed to study nonlinear ship motions (Vinje & Brevig 1981). Both approaches are essentially two-dimensional, corresponding to waves normally incident upon the duck string, and comparison of the two sets of results for a duck on a fixed axis shows good agreement.

1. Introduction

Over the last decade a lot of interest has centred on the possibility of extracting energy from ocean waves. A number of devices have been developed in Britain and elsewhere (see e.g. Cottrill 1981) that can be divided into three categories: (i) terminators – devices that absorb energy from beam seas; (ii) attenuators – devices that absorb energy from head seas; (iii) point absorbers – devices that couple to a wave-frontage larger than their geometric cross-section. In each category the device may be either submerged or surface-piercing; and, since each device has its own merits and drawbacks, it is not yet clear which, if any, of the devices will prove to be economically viable. However, one of the most promising and most developed of the devices is Salter's duck (see figure 1), which belongs to the terminator class of surface-piercing devices. Such devices have special mathematical and experimental appeal, since the main features of their behaviour may be deduced from two-dimensional analysis or testing in a narrow tank.

From the hydrodynamic point of view there seem to be two main problems in wave energy: efficiency under normal operating conditions and survival under extreme conditions. The first problem has received considerable attention for all three categories of device; for the duck, experimental values of the efficiency over a wide range of mixed sea states have been determined when the duck is controlled in all three modes of motion, nod, heave and surge (see Edinburgh Wave Power Project 1978*a*;

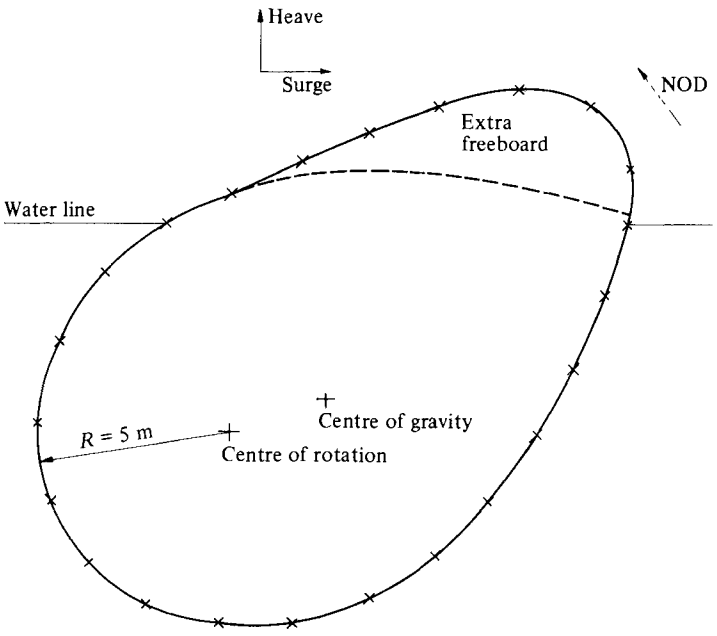

FIGURE 1. Duck geometry and nodal-point distribution (×).

Salter 1979; Greenhow 1980*a*). Corresponding theoretical results using linearized hydrodynamics and a hybrid finite-element scheme have been published by Mynett, Serman & Mei (1979) and extended by Greenhow (1981), where the comparison with experiments in small monochromatic waves was good.

As the wave height increases, nonlinear effects become important, and the efficiency of the device will fall in general. This complicated effect has at least three components:

(i) turbulent flow around the beak of the duck;

(ii) nonlinearity in the buoyancy-restoring force in the nod mode;

(iii) nonlinear hydrodynamic effects resulting in second-harmonic wave generation.

These effects have been studied by Greenhow (1980*b*) where it was shown that the first two effects can be avoided by adding more freeboard to the duck (see figure 1). The improvement in efficiency in the larger waves is very encouraging, and the extra freeboard also simplifies the full-scale design. A further advantage is that we no longer have the sharp beak to contend with in the numerical scheme described below.

The problem of survival in extreme waves, where efficiency is of no consequence, does not appear to have been resolved for many of the devices; most designers envisage submerging their devices to avoid the large slamming forces associated with wave-breaking (see Lighthill 1980) and theoretical work by Brevig, Greenhow & Vinje (1981, 1982) has examined the extreme wave forces on a number of submerged devices. If, however, a surface-piercing device is allowed to yield to the wave, the forces may be considerably lower than for a fixed device. For the duck this is achieved primarily by capsize, the centre of gravity being chosen so that the duck will recover its operating position after the wave has passed. Model tests, conducted in a narrow tank at the University of Edinburgh in 1978, are here described for a duck on a fixed axis.

Although Longuet-Higgins (1981) has made considerable progress with developing an analytic model of a breaking wave, the analysis of the duck/extreme-wave inter-

action is undoubtedly very complex. We therefore extend the numerical nonlinear time-stepping scheme of Longuet-Higgins & Cokelet (1976) to study this case for a duck in finite-depth water, using programmes originally developed for ship-motion problems by Vinje & Brevig (1981). Comparison of the wave-only problem, with no body in the water, and the experimental extreme wave in the model tests has already been made (see Brevig *et al.* 1981). Further, McIver & Peregrine (1981) compare the results of the present method for a breaking wave (see Vinje & Brevig 1980*a*) with the results of Longuet-Higgins & Cokelet (1976) and find good agreement. This paper compares the nonlinear wave and duck motions of the theoretical and experimental results until the wave breaks, and provides a useful check for further work on ship-capsize problems.

2. Details of the experiments

The experimental work took place in the Edinburgh Wave Power Project's 'narrow tank', using a 10 cm diameter model and an 'absorbing' wavemaker controlled by a digital computer. The tests were designed to analyse the response of a model Salter's duck to a deep-water plunging breaker with a steepness ratio of 4·6 to 1. As well as directly measuring model motion and forces transmitted to the support linkage, a series of photographic sequences illustrated the relative motion of model and water.

The equipment

The tank was 9·14 m long by 0·3 m wide, and with a water depth of 0·6 m. The model (symmetrical profile, 10 cm stern diameter, 12 cm axis to nose) was ballasted and trimmed as for energy-extraction experiments. At an axis depth of 6·5 cm and with the centre of gravity below the line of symmetry it recovered unaided from backward capsize. The model was supported by the 'surging–heaving rig', an apparatus allowing easy variation of compliance, damping and inertia separately in the vertical and horizontal planes, by physical and electronic control. For the tests discussed here, the rig was locked to provide an unyielding model axis. However, strain gauges attached to the rig linkages provided measurements of the forces transmitted between this and the fixed reference.

The wavemaker was of the 'absorbing' type (Salter 1978), utilizing force and velocity feedback, and was able to reproduce large-amplitude wave sequences with excellent repeatability in conditions of significant reflection from the model (see figure 5). A Plessey 'Miproc' computer drove the wavemaker through a digital-to-analogue converter 'sample-and-hold' circuit, current amplifier and DC motor. The sampling rate was 20 Hz and the drive was computed as the instantaneous sum of 32 equal-amplitude sinusoidal components with linear frequency increments in the range 0·66–1·27 Hz, each being a submultiple of the computer clock frequency. The phase of each sinusoidal component, at start-up, was calculated so that the crests of each of the tank wavetrains would coincide at the nominal model position, a chosen time after start-up (usually 10 s). This technique of producing a very steep wave by linear superimposition requires precise knowledge of the wavemaker transfer function.

Behind the model, at the other end of the tank, a vertical wedge of densely packed 'Expamet' (perforated aluminium foil) acted as beach.

Before positioning the model, wave measurements were made at the axis position using a compensated conductivity probe.

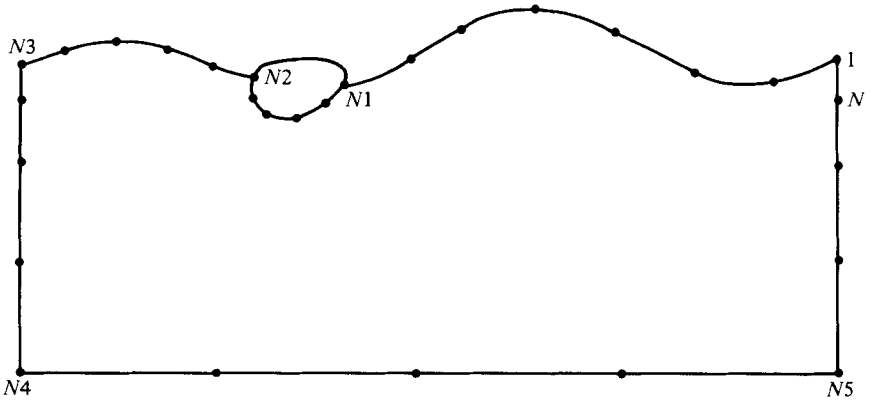

FIGURE 2. Nodal-point distribution for numerical scheme (typically $N1 = 60$, $N2 = 75$, $N3 = 85$, $N = 110$).

Photography

The good repeatability of the system allowed photographic sequences to be compiled from separate stills taken singly on different runs of the wave each time with an increasing delay after start-up. We used a conventional 35 mm camera with an electrically operated shutter.

To freeze motion, electronic flashlights were used for illumination. These had flash durations of less than 2 ms. Three of them illuminated the wave from below, through the glass bottom of the tank (an invaluable aid in showing up the meniscus) and two lit the model from near the camera position.

The camera and lights were controlled by a timer which was set by a computer signal at start-up. This supplied a light control pulse, which was accurate to 1 ms, and it provided an earlier pre-trigger signal to the camera shutter, ensuring that it was open in time for the exposure.

3. Mathematical formulation

As mentioned in § 1 this work is an extension of the numerical scheme described by Vinje & Brevig (1981), and consequently we confine ourselves here to an outline of the theory only. In that paper it was pointed out that for highly transient problems like wave-breaking and capsize it suffices to examine an initial-value problem with the wave profile specified only over a small number of wavelengths (typically one or two wavelengths). If the initial conditions are properly chosen then we may apply periodicity in space to enable the entire semi-infinite fluid to be treated nonlinearly, rather than matching the wave at the boundary to an incident linear wave (see figure 2).

We treat the problem in a mixed Eulerian/Lagrangian description by following the fluid particles forward in time, except along the body, where a modified Lagrangian description is used that follows points fixed to the body surface. Under the usual assumptions of homogeneous, incompressible and irrotational flow we may admit the two-dimensional complex velocity potential:

$$\beta(z,t) = \phi(x,y;t) + i\psi(x,y;t), \tag{3.1}$$

where $z = x+iy$, and ϕ and ψ are respectively the velocity potential and stream function.

The initial values are specified by the velocity potential and elevation on the free surface and the position and velocity of the body (see § 5). Since $\beta(z,t)$ is analytic in the fluid domain, then Cauchy's theorem is valid:

$$\oint_C \frac{\phi+i\psi}{z-z_0}dz = 0, \tag{3.2}$$

where C is a closed contour consisting of the wetted body surface, the bottom, the free surface and two vertical boundaries over which periodicity is applied. z_0 is a point situated outside the contour C.

Evidently applying periodic boundary conditions cannot be entirely correct, since reflection from the duck will not be accounted for properly. We argue that, since the wave-breaking to be examined is a highly transient problem, the local field around the duck may not be significantly affected by the periodicity before the wave breaks and the theory becomes invalid.

The contour C is assumed to consist of two parts: C_ϕ, where ϕ is known, and C_ψ, where ψ is known. This gives rise to two Fredholm's equations of the second kind:

$$\alpha\psi(x_0,y_0,t) + \mathscr{R}\int_C \frac{\phi+i\psi}{z-z_0}dz = 0 \tag{3.3}$$

for $z_0 \in C_\phi$, and

$$\alpha\phi(x_0,y_0,t) + \mathscr{R}\int_C \frac{\phi+i\psi}{z-z_0}dz = 0 \tag{3.4}$$

for $z_0 \in C_\psi$. Here α is the angle between the two tangents of C at z_0 (equal to π for any smooth part of C).

On the free surface ϕ is given as an initial condition, and hence this is part of C_ϕ. The bottom forms a streamline, and accordingly is part of C_ψ. On the vertical boundaries both ϕ and ψ are unknown, but the periodicity requirement provides the necessary additional equations needed to solve the system. For a duck on a fixed axis, Vinje & Brevig (1980*b*) give the value of ψ on the wetted surface as

$$\psi = -\tfrac{1}{2}\dot{\theta}\xi\xi^*, \tag{3.5}$$

when θ is the nod angle measured in the anticlockwise direction and ξ is the coordinate of the point on the body measured with respect to axes at the centre of rotation (equal to the centre of gravity for ships but not for ducks). Thus according to (3.5) the wetted body surface forms part of C_ψ.

To step forward in time we notice that since $\partial\beta/\partial t$ is also an analytic function in the fluid domain then (3.3) and (3.4) will be valid with $\partial\phi/\partial t$ and $\partial\psi/\partial t$ replacing ϕ and ψ respectively. On the free surface we have the kinematic boundary condition

$$\frac{Dz}{Dt} = u+iv \equiv w^*, \tag{3.6}$$

which yields the new surface elevation. The dynamic boundary condition

$$\frac{D\phi}{Dt} = \tfrac{1}{2}ww^* - gy - P_s/\rho \tag{3.7}$$

gives the new value of ϕ on the free surface. In the above equations

$$\frac{D(\,)}{Dt} = \frac{\partial(\,)}{\partial t} + \nabla\phi\,.\,\nabla(\,) \tag{3.8}$$

is the material derivative, (u, v) is the velocity of the particles, g is the acceleration due to gravity, ρ is the density of water and P_s is an arbitrary applied pressure which is set equal to zero in this paper. Also

$$w = u - iv = \frac{\partial \beta}{\partial z} \tag{3.9}$$

gives the fluid-particles' velocities.

To evaluate the pressure and hence the forces on the body we use

$$-\frac{p}{\rho} = \frac{\partial \phi}{\partial t} + \tfrac{1}{2} w w^* + gy, \tag{3.10}$$

and hence we need to know $\partial\phi/\partial t$ on the body, which requires solving Cauchy's equation for $\partial\beta/\partial t$. On the free surface we have

$$\frac{\partial \phi}{\partial t} = -\tfrac{1}{2} w w^* - gy, \tag{3.11}$$

whilst on the bottom $\partial\psi/\partial t$ is known, and periodicity is again used on the vertical boundaries. This leaves $\partial\psi/\partial t$ to be calculated on the body, for which Vinje & Brevig (1981) give the formula

$$\frac{\partial \psi}{\partial t} = -\tfrac{1}{2}\ddot{\theta}\xi\xi^* - \mathscr{R}\{\xi w \dot{\theta}\} \tag{3.12}$$

for a duck on a fixed axis. We see that the unknown acceleration $\ddot{\theta}$ has been factored out, and we proceed to solve the compound problem

$$\frac{\partial \psi}{\partial t} = \ddot{\theta}\frac{\partial \psi_3}{\partial t} + \frac{\partial \psi_4}{\partial t} \tag{3.13}$$

on the body (the notation is chosen to correspond to that of Vinje & Brevig (1981)). Comparison of (3.12) and (3.13) yields $\partial\psi_3/\partial t$ and $\partial\psi_4/\partial t$ on the body, whilst on the free surface $\partial\phi_3/\partial t = 0$, and $\partial\phi_4/\partial t$ is given by (3.11). Solving Cauchy's equation for the two component problems gives the total solution as

$$\frac{\partial \beta}{\partial t} = \frac{\partial \beta_3}{\partial t}\ddot{\theta} + \frac{\partial \beta_4}{\partial t}. \tag{3.14}$$

Substituting the solutions of $\partial\beta_3/\partial t$ and $\partial\beta_4/\partial t$ into (3.10) gives the pressures p_3 and p_4 associated with each potential, where

$$p_3 = -\rho\frac{\partial \phi_3}{\partial t}, \quad p_4 = -\rho\frac{\partial \phi_4}{\partial t} - \tfrac{1}{2}\rho w w^* - \rho g y. \tag{3.15}$$

Integration over the body surface then yields the equation of motion for a duck of inertia I and mass m, as

$$\left[I + \mathscr{R}\int_{\text{body}} p_3 \xi\, dz\right]\ddot{\theta} = -\mathscr{R}\int_{\text{body}} p_4 \xi\, dz + mg\mathscr{R}(\xi_G) \tag{3.16}$$

from which the acceleration can be found. Here ξ_G is the position of the centre of gravity relative to the position of the centre of rotation. We use the solution of (3.16), (3.6) and (3.7) to step forward in time, giving the new body velocity, free-surface

elevation and velocity potential on the free surface. This establishes a new set of initial conditions for the new time from which we can solve for the complex velocity potential β and repeat the process described above.

4. Numerical solution

To solve Cauchy's equations for β and $\partial\beta/\partial t$ we assume a linear variation of these functions between the nodal points on C shown in figure 2. The influence function of these variables at the point z is therefore

$$\left.\begin{aligned} \Lambda_j(z) &= \frac{z-z_{j+1}}{z_j-z_{j+1}} \quad \text{for } z \text{ on } C \text{ between } z_j \text{ and } z_{j+1}, \\ \Lambda_j(z) &= \frac{z-z_{j-1}}{z_j-z_{j-1}} \quad \text{for } z \text{ on } C \text{ between } z_{j-1} \text{ and } z_j, \end{aligned}\right\} \tag{4.1}$$

and zero elsewhere on C. Introducing this influence function into Cauchy's equation (3.2) gives the following matrix equation:

$$\oint_C \frac{\phi+i\psi}{z-z_k} \simeq \sum_j \Gamma_{kj}\beta_j = 0, \tag{4.2}$$

and a similar equation for $\partial\beta_j/\partial t$, where $\beta_j = \beta(z_j, t)$. Furthermore,

$$\Gamma_{kj} = \frac{z_k-z_{j-1}}{z_j-z_{j-1}} \ln\frac{z_j-z_k}{z_{j-1}-z_k} + \frac{z_k-z_{j+1}}{z_j-z_{j+1}} \ln\frac{z_{j+1}-z_k}{z_j-z_k}, \tag{4.3}$$

with limiting values applied when $k = j-1, j$ or $j+1$.

If

$$\epsilon = \frac{z_{j-1}-z_j}{z_j-z_k}, \quad \delta = \frac{z_{j+1}-z_j}{z_j-z_k} \tag{4.4}$$

are both small ($< \epsilon_1$) then

$$\Gamma_{kj} \simeq \tfrac{1}{2}(\delta-\epsilon)[1-\tfrac{1}{3}(\delta+\epsilon)], \tag{4.5}$$

an approximation that reduces the cost of running the program by about 40 %, whilst the accuracy is not significantly affected. We choose $\epsilon_1 = 0{\cdot}2$ until any part of the wave profile becomes vertical when $\epsilon_1 = 0{\cdot}1$. Otherwise we use the exact expression of (4.3).

To ensure that we obtain Fredholm integral equations of the second kind we rewrite (4.2) as

$$\mathscr{R}\left\{\sum_{j=1}^{N} \Gamma_{kj}\beta_j\right\} = 0 \tag{4.6}$$

when z_k is on C_ϕ, and

$$\mathscr{R}\left\{i\sum_{j=1}^{N} \Gamma_{kj}\beta_j\right\} = 0 \tag{4.7}$$

when z_k is on C_ψ.

When z_k is on the vertical boundaries then ϕ and ψ are both unknown. We can, however, sum appropriate rows in the matrix equations (4.6) and (4.7) (row k and its corresponding row on the other vertical boundary). Using the assumed periodicity of the solution, we thus eliminate some of the unknowns, achieving the correct number of equations. We obtain a set of equations of the form $\mathbf{Ax} = \mathbf{b}$, where $\mathbf{A}$ depends

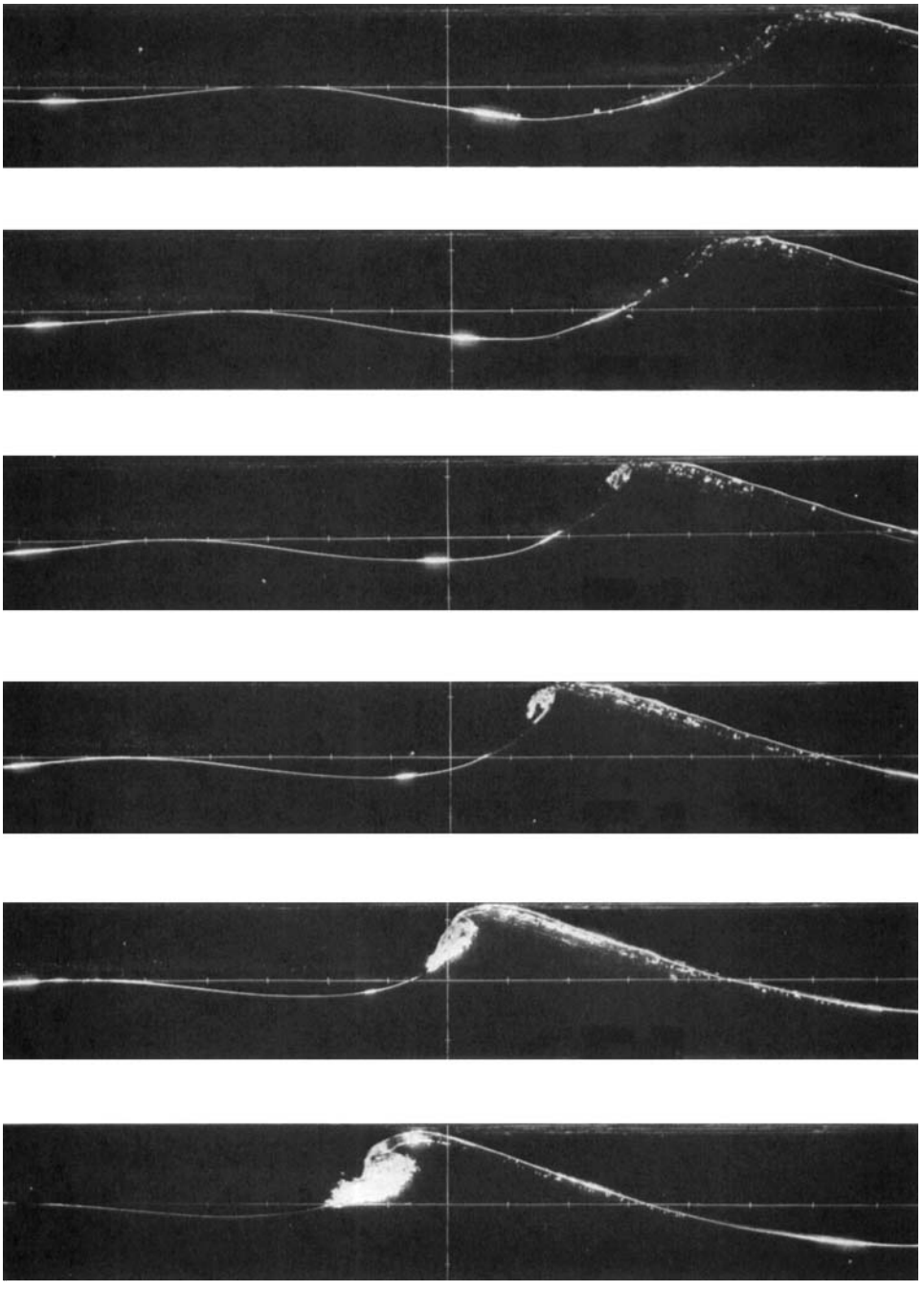

(*a*)

FIGURE 3(*a*). For caption see opposite.

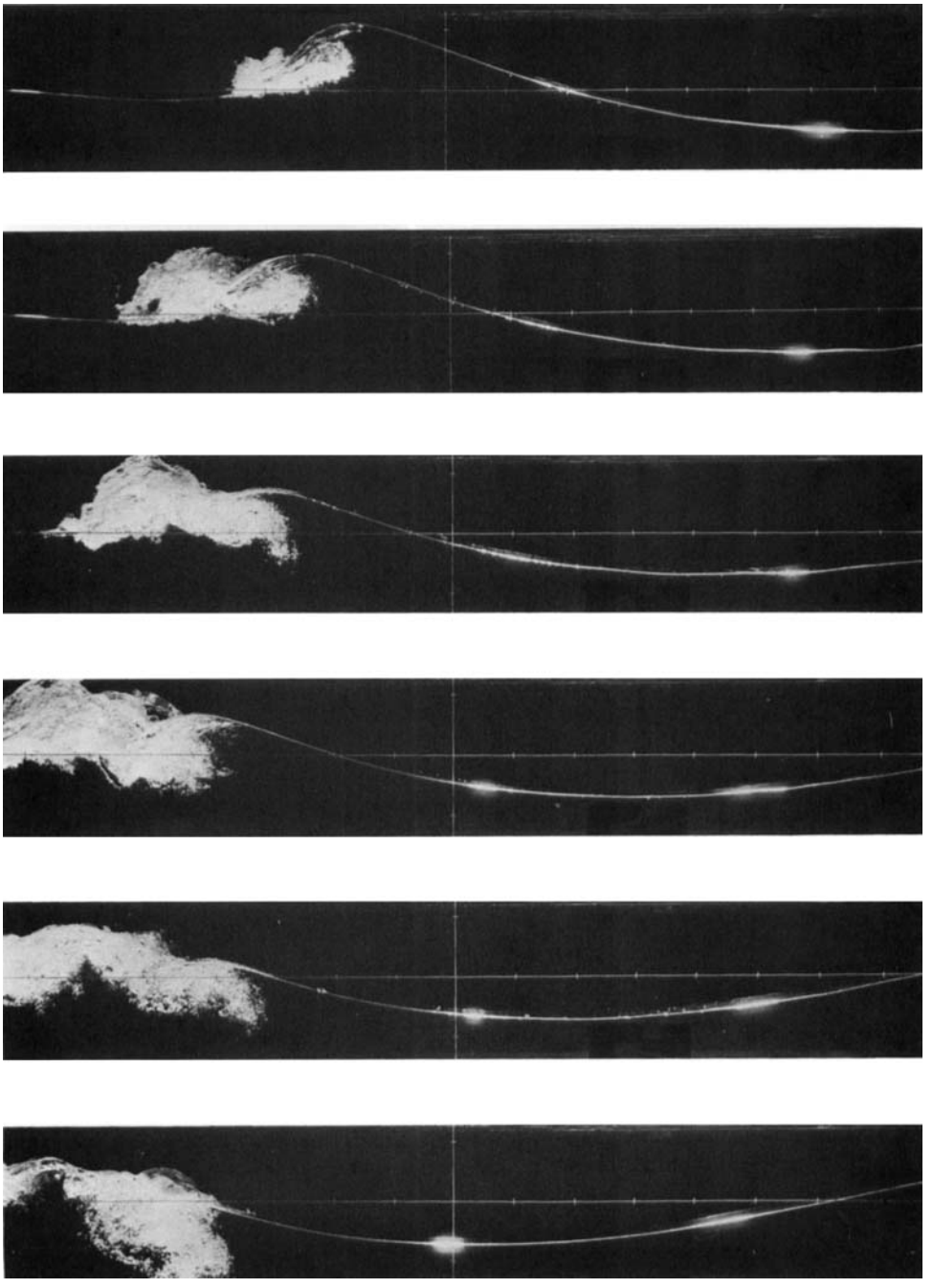

(*b*)

FIGURE 3. Time progression of the experimental breaking wave. At full scale the tick marks on the axes indicate 10 m intervals, and the time between successive photographs is 0·816 s.

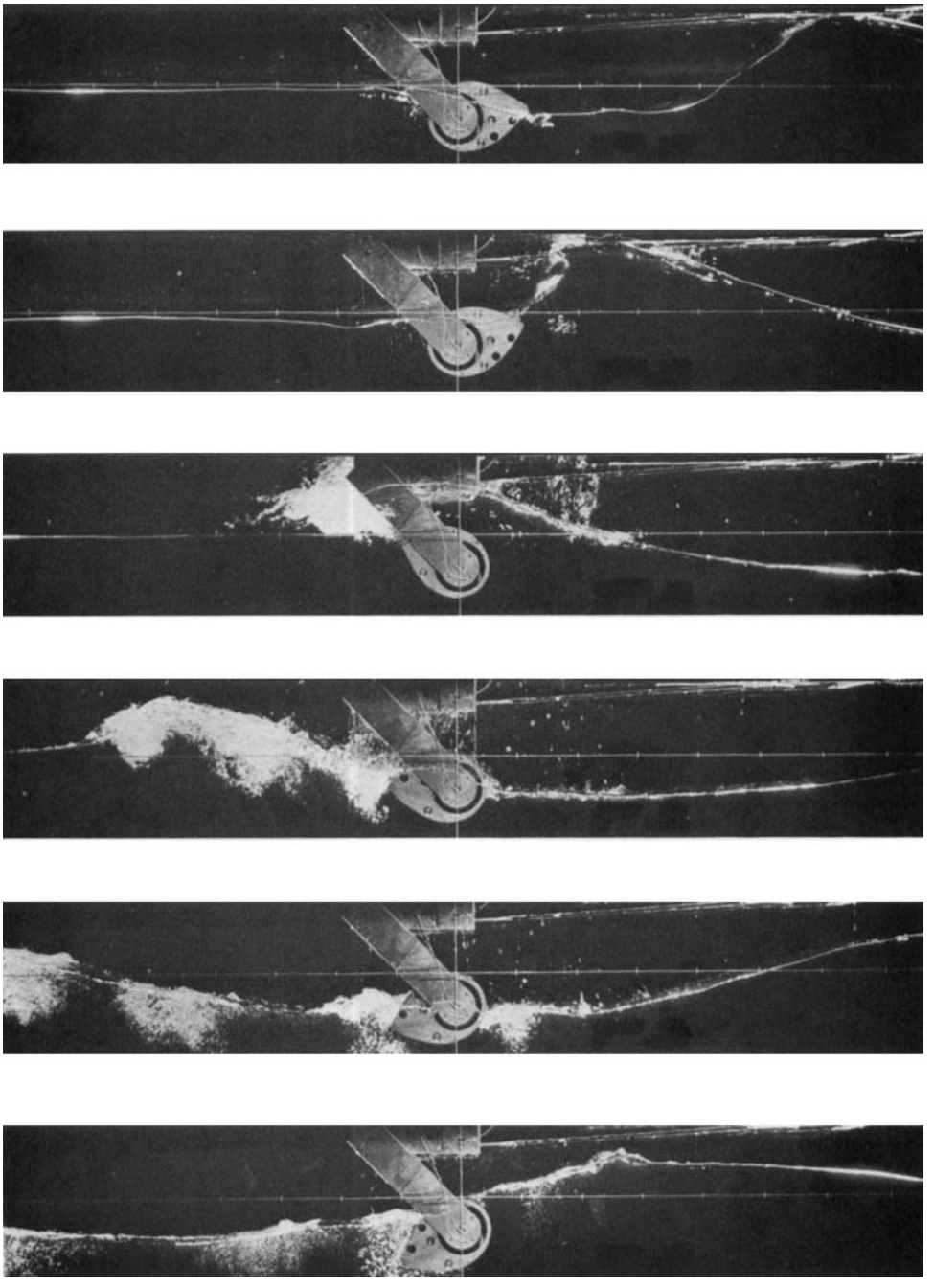

(*a*)

FIGURE 4(*a*). For caption see opposite.

only on the shape of the control surface and therefore can be retained for calculating the complex-potential derivatives $\partial\beta_3/\partial t$ and $\partial\beta_4/\partial t$.

To find the fluid velocities w given by (3.9), β is differentiated using a second-order central-difference scheme. The free-surface elevation, velocity potential and body velocity are stepped forward in time using the Runge–Kutta method for the first

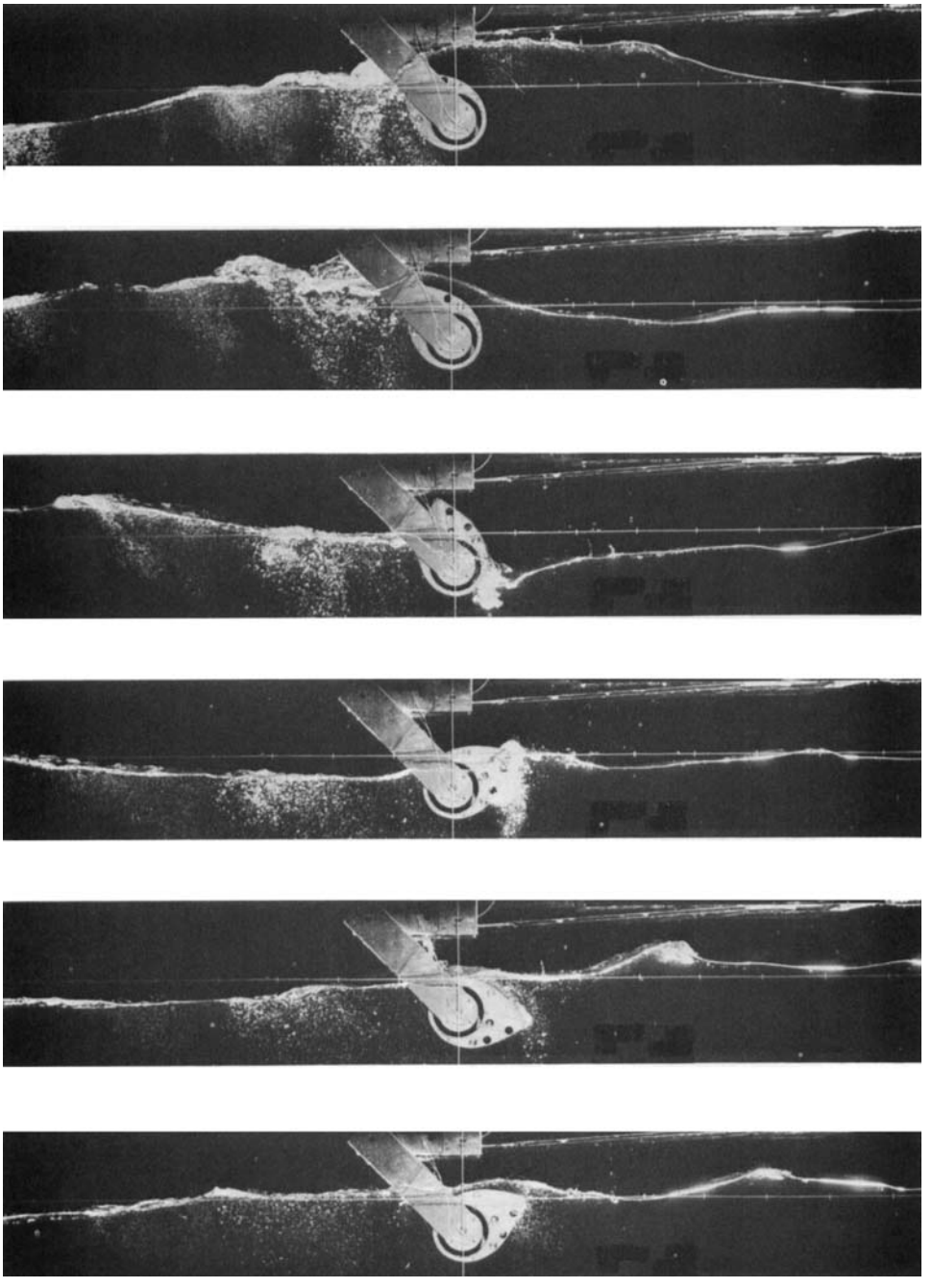

(*b*)

FIGURE 4. Duck capsize in breaking wave and recovery.

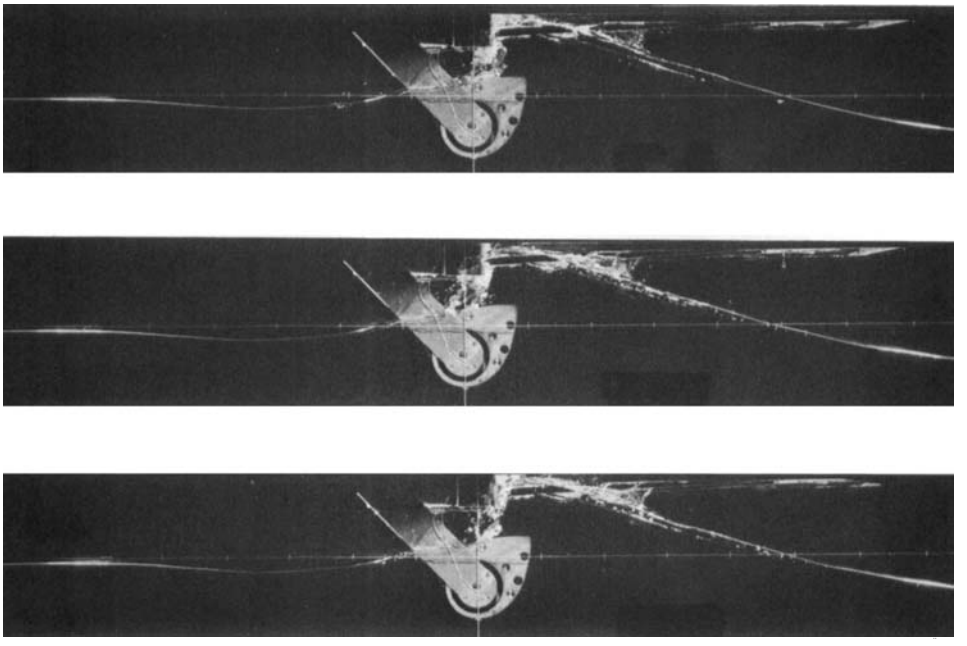

FIGURE 5. Repeatability; three separate runs have been photographed at the same instant.

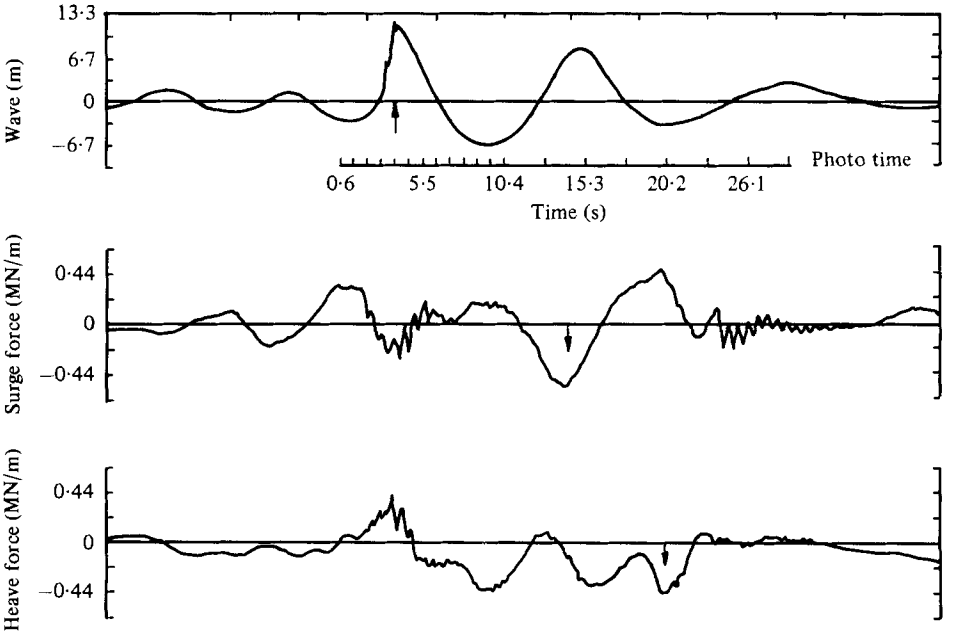

FIGURE 6. Wave and force measurement for undamped duck on fixed axis scaled to full-sized 10 m rear duck diameter. Arrows indicate maximum absolute values.

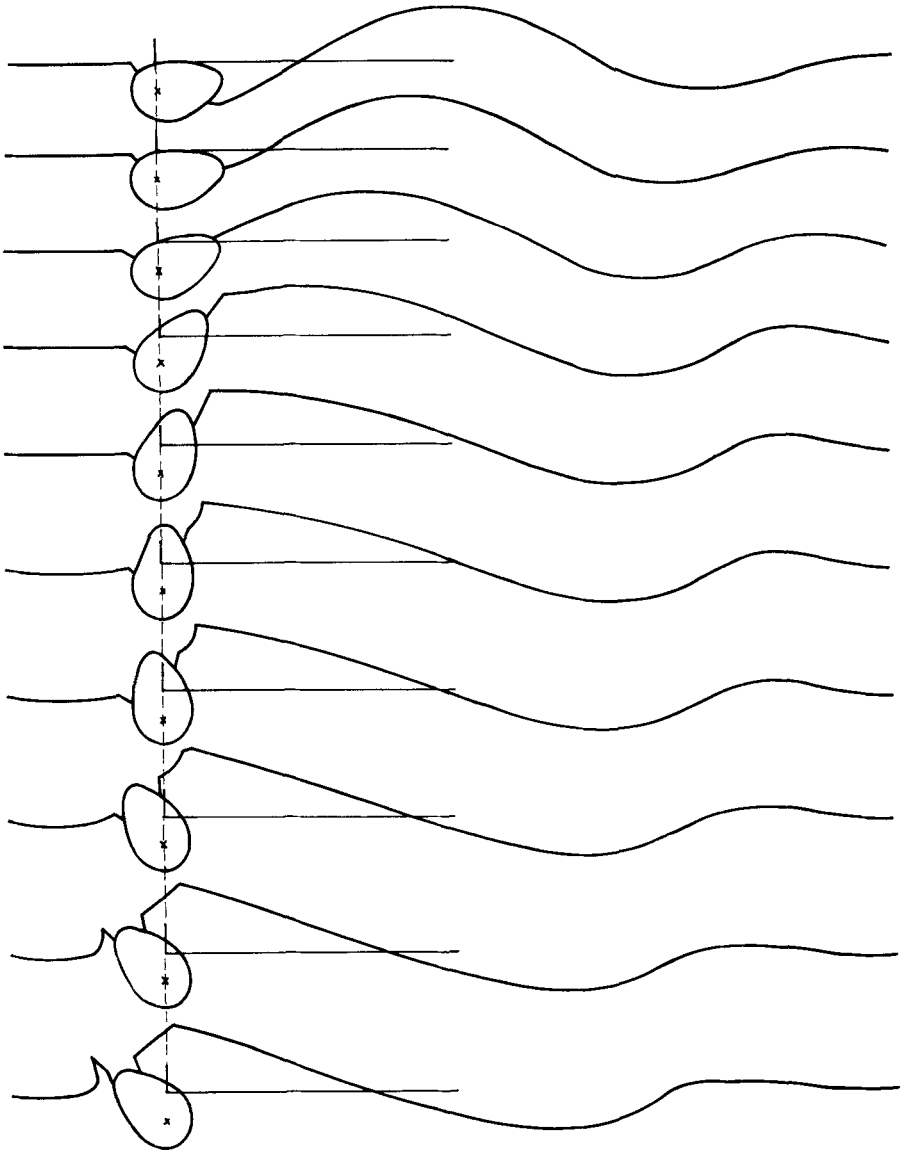

FIGURE 7. Computer simulation of duck capsize in non-breaking wave.

three time steps, after which we use Hamming's fourth-order predictor–corrector method which utilizes information from the previous three time steps. The necessary time derivatives are furnished respectively by (3.6), (3.7) and (3.16).

For surface-piercing bodies we have a particular problem with the points of intersection of the free surface with the body. Depending upon the angle of intersection of the body and free surface, the velocity w may be singular. Another possibility is that the gradient of ψ along the body does not match the gradient of ϕ on the free surface, causing a weaker type of singularity. Furthermore, even in the absence of any singularity the gradient of the velocity field may become large, making the numerical solution difficult. In the absence of any satisfactory answer to these problems we appeal to the visual evidence of the photograph sequence of figure 8. It

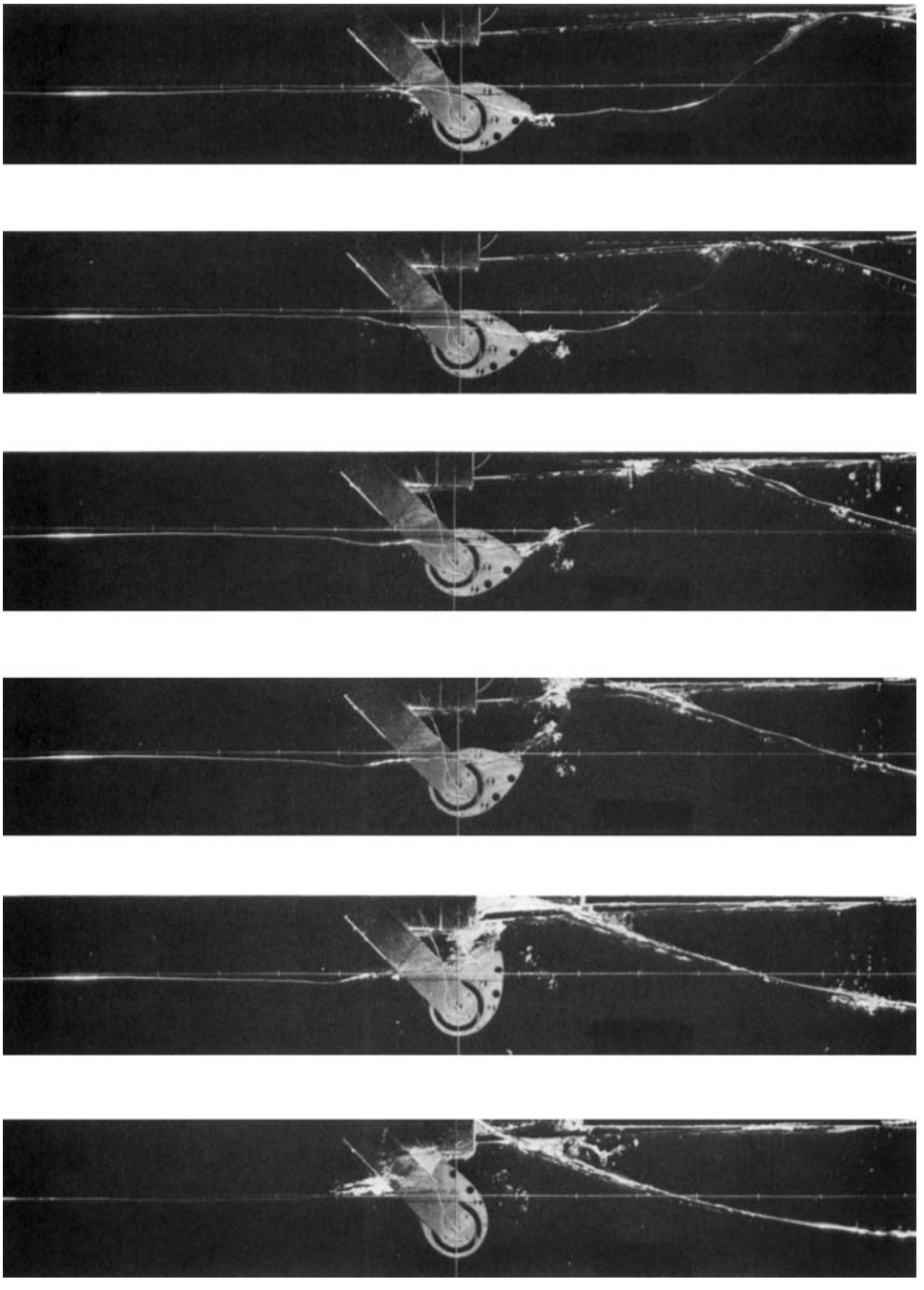

(*a*)

FIGURE 8 (*a*). For caption see opposite.

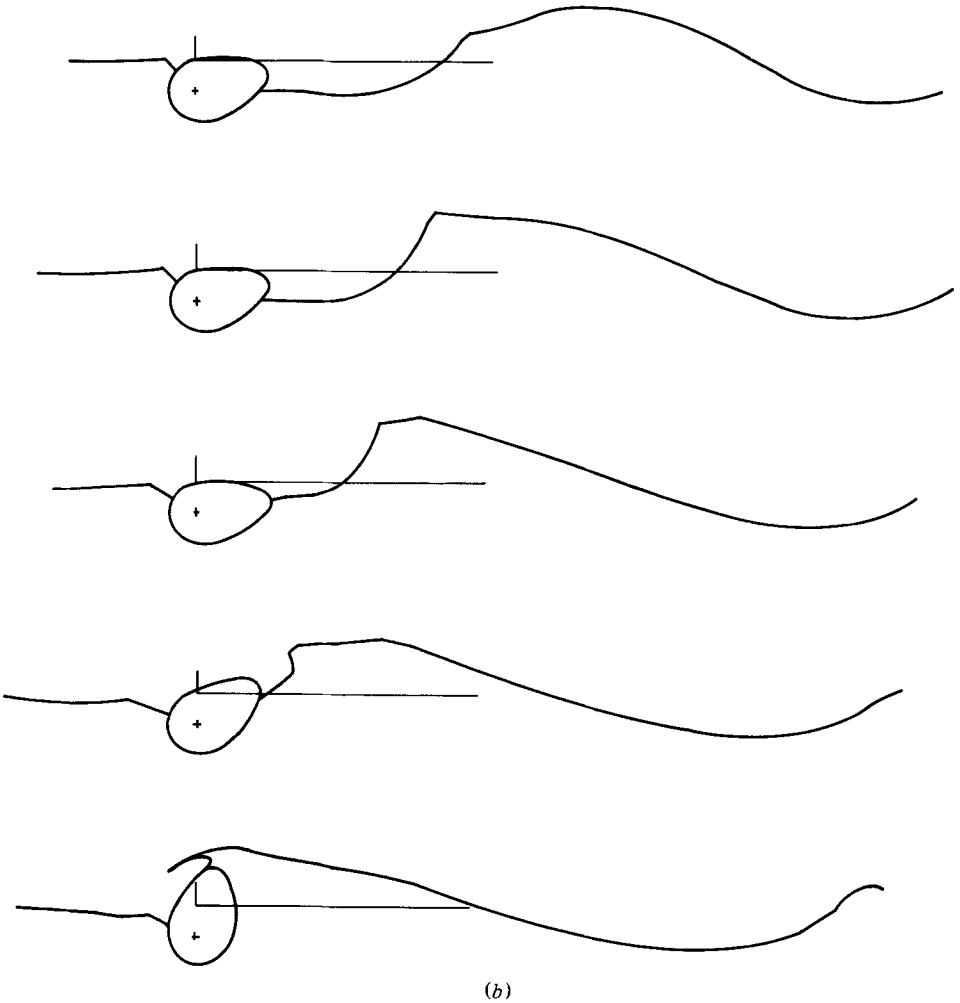

(*b*)

FIGURE 8. Comparison of experimental and theoretical results for duck capsize in breaking wave up to the point of breaking. (We suggest superposing two Xerox transparencies of these results for comparison.)

would seem that for the duck-capsize problem a good algorithm for calculating the position of the point of intersection is to draw a straight line from the neighbouring point on the free surface to the centre of rotation. The intersection point thus generated is regarded as being on C_ψ for the calculation of the complex velocity potential, rather than on C_ϕ.

From the point of view of the numerical solution it is vital to ensure that the nodal-point spacing along the free surface does not change too rapidly in space. Therefore it is sometimes necessary to remove or introduce points at certain times during the calculation. When points are introduced a linear variation in position and velocity potential is assumed between the neighbouring points.

5. Results and discussion

For comparison with figure 4, figure 3 shows the narrow-tank extreme wave used in the experimental tests without the duck in the water. A comparison of this wave

with a corresponding theoretical wave has been made by Brevig *et al.* (1981), where the agreement between the time progression of the two waves is fair, the differences being due to the method of generation of the experimental wave differing from the sinusoidal wave used as the initial condition for the theoretical wave. In this paper we present more realistic initial conditions suggested by the start of the photograph sequence shown in figure 4. Here the duck has been positioned in the water at the nominal breaking point of the wave (as if the duck were absent) and held on a fixed axis. The sequence shown in figure 4 is in fact made up from separate runs of the wave, taking one photograph per run. This requires good repeatability of the wave profile, which is demonstrated by comparing the photographs of figure 5 where three separate runs are photographed at a particular instant.

From a series of extensive tests undertaken at the University of Edinburgh in 1978 (see Edinburgh Wave Power Project 1978*b*) we know that an undamped duck on a rigid axis will have higher angular velocities, and consequently greater angular displacements than those of ducks on a compliant axis. Therefore we regard the undamped duck on a rigid axis as a good check for the theory.

Figure 6 presents measurements of the wave profile without the duck, and the forces on the axis in the heave-and-surge direction. The sign convention is positive upwards for heave, positive opposite the wave direction for surge, and positive anticlockwise for nod.

Before we start the time-stepping we need to provide the following initial conditions: wave elevation and velocity potential on the free surface, and position and velocity of the body. In principle it should be possible to start the body from rest in locally calm water with an incident wave some distance from the body; in practice this would require prohibitive amounts of computer storage and time to run a wave break. We therefore obtain initial conditions from the photographs just before the wave break as described below.

Figure 7 shows theoretical results for initial conditions as follows: the centre of gravity, mass and moment of inertia are taken from experimental data; the initial displacement and velocity is taken from the photographs ($\dot{\theta} = 0$); behind the duck the wave elevation and velocity potential are taken to be zero; the incident wave is given from linear theory for deep water waves (wavelength 110 m, crest-to-trough height 20 m and water depth 60 m, corresponding closely to the experimental wave); at distances greater than $\frac{3}{4}$ wavelength from the duck the elevation and velocity potential on the free surface is decreased linearly with distance to zero at $\frac{5}{4}$ wavelengths from the duck. Thus we are able to apply periodic boundary conditions over this control volume. Returning to figure 7, we see that the duck capsizes fully during the sequence, and the numerical solution breaks down because the duck submerges. Comparison with the sequence of photographs of figure 4 shows that the duck velocities and positions look correct, but the wave profile generated by the above initial conditions is incorrect and does not lead to the spilling breaker seen in the experiments, but rather simulates duck capsize in large but non-breaking waves. Furthermore, the sharp corners in the free surface are almost certainly due to the numerical scheme used, and more especially to the placing of the point of intersection of the body and the free surface.

We refine the initial conditions as shown in figure 8, where the control volume length is increased to $\frac{7}{4}$ wavelengths, and the linear decrease is applied both behind and in

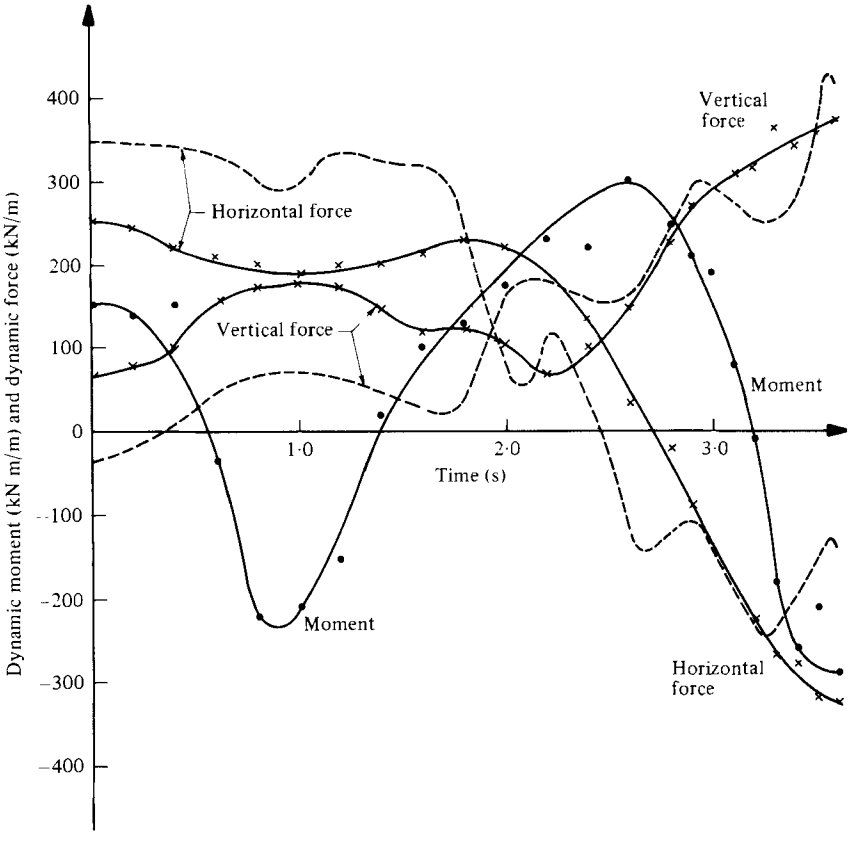

FIGURE 9. Dynamic axis forces and duck moment for capsize in breaking wave: ——, theory; – – –, experiment.

front of the crest. This wave profile corresponds closely to the experimental wave profile in the region of the duck, and a comparison of the theory and experiments is shown in figure 8 as the wave progresses up to the point of breaking. The overall agreement is excellent, although a slight discrepancy in the duck position arises at the end of the calculation, the theory giving larger duck angular displacements than the experiment. Possible causes for this are numerical inaccuracy in the force calculations, choice of initial conditions and the extra freeboard added in the theory, and spray formation, turbulence and friction in the experiments. With regard to the free-surface elevation it is not clear where green water ends (the theoretical free surface) and spray begins in the later stages of the wavebreak. We conclude that the agreement is about as good as we can expect from the theory, which leaves out spray formation.

Finally, a comparison of the theoretical and experimental values of the forces on the axis is given in figure 9, whilst figure 10 gives the angular displacements, velocities and accelerations. The comparison of the forces is quite good until just before the wave break, when the theory becomes unreliable. Despite this, the angular displacements, which are smoothed over time, may still be fairly accurate. (The fast oscillations in the experimental forces shown in figures 6 and 10 are due to vibration in the rig, and are not hydrodynamic in origin.) It is natural to ask whether the forces calculated from linearized theory by Mynett *et al.* (1979) have any validity in breaking

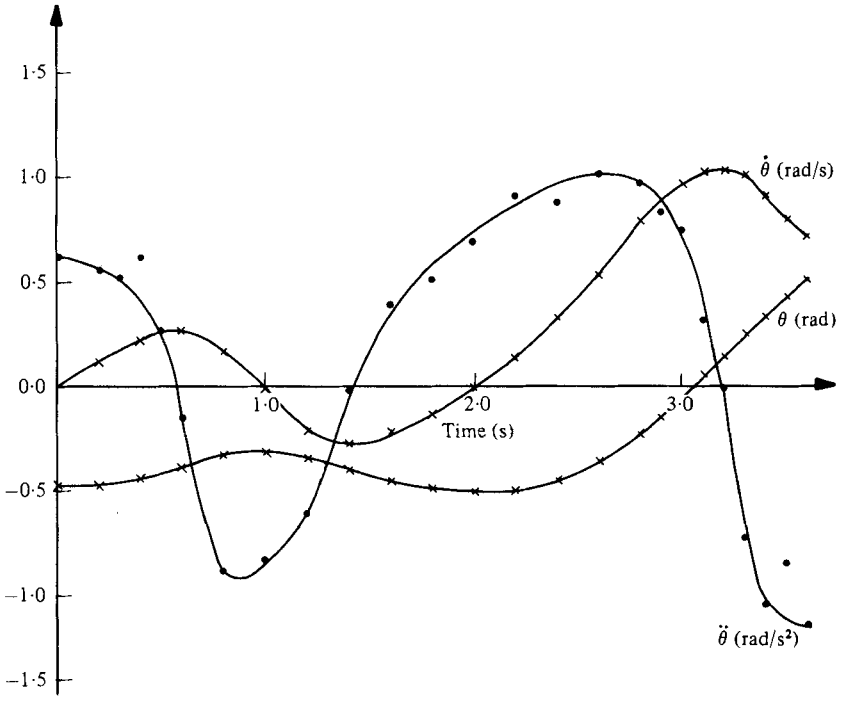

FIGURE 10. Angular displacement, velocity and acceleration for capsize in breaking wave.

waves. We would regard a comparison of the two sets of results as misleading, since the linearized theory deals with steady-state forces, whereas the present theory relies, through the assumption of periodicity, on the highly transient nature of the problem. Work is currently under way to replace the periodicity condition with a vertical boundary condition that matches to an incident wave, whereby a nonlinear steady-state solution could be approached for comparison with linearized theories.

6. Conclusion

The behaviour of Salter's duck in waves of extreme steepness in a narrow tank has been photographed, and the axis forces have been measured. From these measurements the Edinburgh Wave Power Team has concluded that it is possible to engineer a duck that will survive storm conditions off the coast of Scotland and elsewhere.

A two-dimensional theory has been developed giving excellent agreement with the model tests up until the point of wave-breaking. We expect that computer simulations of this type could be a useful tool, not only in the study of the survival of terminator-type wave-power devices, but also for nonlinear ship motions and capsize in beam seas.

A large amount of the programming used was developed under the 'Ships in Rough Seas' project sponsored by The Royal Norwegian Council for Industrial and Scientific Research (NTNF), the Norwegian Fisheries Research Council and the Norwegian Maritime Directorate. One of us (M.G.) wishes to thank NTNF for financial support during this research. The experiments were conducted as part of the Edinburgh

University Wave Power Project sponsored by the U.K. Department of Energy. Finally we would like to thank Mr Stephen Salter for his helpful comments and discussions.

REFERENCES

BREVIG, P., GREENHOW, M. & VINJE, T. 1981 Extreme wave forces on submerged cylinders. In *Proc. B.H.R.A. 2nd Int. Symp. on Wave and Tidal Energy, Cambridge.*

BREVIG, P., GREENHOW, M. & VINJE, T. 1982 Extreme wave forces on submerged wave energy devices. *J. Appl. Ocean Res.* (to appear).

COTTRILL, A. 1981 Wave energy: main U.K. contenders line up for 1982 decision. *Offshore Engineer*, January 1981.

EDINBURGH WAVE POWER PROJECT 1978*a* *Fourth Year Report*, vol. 1.

EDINBURGH WAVE POWER PROJECT 1978*b* *Fourth Year Report*, vol. 2.

GREENHOW, M. 1980*a* Scatter diagram tests for duck and joint power and efficiency. *Edinburgh Wave Power Project. Internal Rep.*

GREENHOW, M. 1980*b* An investigation into the effect of geometrical changes, non-linearities and backbone compliance on the efficiency of Salter's duck in monochromatic and mixed seas: part I. *Edinburgh Wave Power Project Internal Rep.*

GREENHOW, M. 1981 Efficiency calculation for Scatter's duck on a compliant axis. *J. Appl. Ocean Res.* **3**, 145.

LIGHTHILL, J. 1980 Mathematical analysis related to the Vickers project: part I. In *Power from Sea Waves: Proc. I.M.A. Conf. Wave Energy, Edinburgh* (ed. B. Count), chap. III.5. Academic.

LONGUET-HIGGINS, M. S. 1981 Kinematics of breaking waves. In *Proc. Symp. Hydrodynamics in Ocean Engng, Trondheim.*

LONGUET-HIGGINS, M. S. & COKELET, E. D. 1976 The deformation of steep surface waves on water. I. A numerical method of computation. *Proc. R. Soc. Lond.* A **350**, 1.

MCIVER, P. & PEREGRINE, D. H. 1981 Comparison of numerical and analytical results for waves that are starting to break. In *Proc. Symp. Hydrodynamics in Ocean Engng, Trondheim.*

MYNETT, A. E., SERMAN, D. D. & MEI, C. C. 1979 Characteristics of Salter's cam for extracting energy from ocean waves. *J. Appl. Ocean Res.* **1**, 13.

SALTER, S. H. 1978 The development of the duck concept. In *Proc. Wave Energy Conf., London–Heathrow, Nov.* 1978.

SALTER, S. H. 1979 Recent progress on ducks. In *Proc. Wave Energy Utilisation Conf., Gothenberg.*

VINJE, T. & BREVIG, P. 1980*a* Numerical simulation of breaking waves. In *Proc. 3rd Int. Conf. on Finite Elements in Water Resources, Univ. of Miss., Oxford, Miss., May* 1980.

VINJE, T. & BREVIG, P. 1980*b* Nonlinear, two-dimensional ship motions. *S.I.S. Project, NHL and NTH Rep., Trondheim.*

VINJE, T. & BREVIG, P. 1981 Nonlinear ship motions. In *Proc. 3rd Int. Conf. on Numerical Ship Hydrodynamics, Paris.*